Numerical Investigation of the Value Function for the Homicidal Chauffeur Problem with a More Agile Pursuer

Valerii S. Patsko
Institute of Mathematics and Mechanics
S. Kovalevskaya str. 16, 620219
Ekaterinburg, Russia
patsko@imm.uran.ru

Varvara L. Turova
Technical University of Munich
Boltzmannstr. 3, 85747
Garching, Germany
turova@ma.tum.de

Abstract

The paper is devoted to the investigation of a time-optimal differential game in which the pursuer possesses increased control capabilities comparing to the classical homicidal chauffeur problem. Namely, the pursuer steers not only the angular velocity of turn but can additionally change the magnitude of his linear velocity. For such a new variant of the dynamics with non-scalar control of the pursuer, a complete description of families of semipermeable curves is given and the dependence of the structure of level sets of the value function on a parameter that defines the bound on the magnitude of the pursuer's velocity is explored by numerical methods.

Key words. Time-optimal control, pursuit-evasion differential game, value function, semipermeable curves, homicidal chauffeur game, numerical construction.

AMS Subject Classifications. Primary 49N70, 49N75; Secondary 93B40.

1 Introduction

One of the most well-known model problems in the theory of differential games is the homicidal chauffeur problem proposed by R. Isaacs in 1951 (see [9]; [10]). The pursuer P (a car) and the evader E (a pedestrian) are moving in the plane. The dynamics are:

$$\begin{array}{lll} P: & \dot{x}_p = w\sin\theta & E: \quad \dot{x}_e = v_1 \\ & \dot{y}_p = w\cos\theta & \dot{y}_e = v_2 \\ & \dot{\theta} = w\,u/R, \;\; |u| \le 1; & |v| \le \rho. \end{array} \tag{1}$$

P. Bernhard et al. (eds.), *Advances in Dynamic Games and Their Applications*,
Annals of the International Society of Dynamic Games 10, DOI: 10.1007/978-0-8176-4834-3_13,

The linear velocity w of the car is constant. The angular velocity of rotation of the linear velocity vector is bounded, which means that the radius of turn of the car is bounded from below. The minimal turning radius is denoted by R.

The pedestrian is a non-inertial object that can change the value and direction of his velocity $v = (v_1, v_2)'$ instantaneously. The maximal possible value of the velocity is specified.

By a given circular neighborhood of his current geometric position, player P tries to capture player E as soon as possible.

The book by R. Isaacs [10] contains some elements of solution of the homicidal chauffeur problem. A complete solution to the problem is given in works by J. V. Breakwell and A. W. Merz (see [4]; [15]). Some other variants of differential games with the homicidal chauffeur dynamics are investigated in [12]; [5]; [13]; [2]; [6]. In many papers (see, e.g., [1], [19]), the homicidal chauffeur game is used as a test problem for evaluating the efficiency of algorithms for the computation of the value function and optimal strategies.

The dynamics like the ones of player P have very long history beginning with the paper by A. A. Markov [14]. In particular, the model is utilized when considering control problems related to the aircraft motion in a horizontal plane (see, e.g., [18]).

In papers on theoretical robotics, this model of dynamics is often referred to as Dubins' car because the paper [8] contains a theorem on the number and type of switches of the open-loop control that brings the object from a given state with a specified direction of the velocity vector to a terminal state for which the direction of the velocity vector is also prescribed.

By normalizing the time and geometric coordinates, one can always achieve $w = 1$, $R = 1$ in system (1). Therefore, system (1) takes the form

$$\begin{array}{lll} P: & \dot{x}_p = \sin\theta & E: \quad \dot{x}_e = v_1 \\ & \dot{y}_p = \cos\theta & \dot{y}_e = v_2 \\ & \dot{\theta} = u, \ \ |u| \le 1; & |v| \le \nu. \end{array} \tag{2}$$

Recent theoretical works on controlled cars use intensively the following dynamics (see [20]; [11]):

$$\begin{aligned} &\dot{x}_p = w\sin\theta \\ &\dot{y}_p = w\cos\theta \\ &\dot{\theta} = u \\ &|u| \le 1, \ \ |w| \le 1, \end{aligned} \tag{3}$$

in which the car has two controls. The first control u steers the forward motion direction $h = (\sin\theta, \cos\theta)'$ of the car. The second control w changes the magnitude of the linear velocity instantaneously. The velocity vector is directed along h for $w > 0$, and opposite to h for $w < 0$. If $w = 0$, the object remains immovable. Of course, instantaneous change of the velocity is a mathematical idealization. But

following [20], p. 373, "for slowly moving vehicles, such as carts, this seems like a reasonable compromise to achieve tractability".

In papers on robotics, model (3) is called Reeds and Shepp's car. Time-optimal problems with Reeds and Shepp's dynamics were considered in [20], [24], [3], [22], [25], [23].

It seems quite natural to consider differential games where the pursuer has additional control capabilities comparing with dynamics (2). Namely, the pursuer can instantaneously change the value of his linear velocity within some bounds. In other words, Isaacs-Dubins' car turns into Reeds-Shepp's type car. The present paper is devoted to the investigation of such a differential game.

The purpose of this paper is to give a complete description of families of semipermeable curves for the problem considered and construct level sets of the value function by numerical methods. In the paper [16], a similar investigation is done by the authors for the classical homicidal chauffeur problem as well as for an "acoustic" variant of the dynamics and for a conic surveillance-evasion game. The present work continues the investigation in [16]. The difference is that, for the first time, non-scalar control of the pursuer in the homicidal chauffeur game is considered. This makes the families of semipermeable curves and the structure of level sets of the value function more complicated.

In papers on theoretical robotics, considerable attention is devoted to the analytical description of the boundary of reachable sets in the plane of geometric coordinates for Dubins' car model (i.e., $a = 1$) and for Reeds and Shepp's model (i.e., $a = -1$) (see [7], [21], [25], and references herein). Results on the construction of level sets of the value function presented in the paper can be interpreted as a description of time-limited game reachable sets for a car with a given range of the instantaneous change of the linear velocity magnitude. During the process of motion, the car is subjected to a dynamic non-inertia disturbance that can distort the velocity vector within prescribed bounds. If this disturbance becomes vanishing small, the game reachable sets are transformed into usual reachable sets for the control problem in the absence of disturbances. But even for $a = 1$ and $a = -1$ the analytical description of these sets is not simple. The authors do not know any papers that study reachable sets for $a \neq \pm 1$, and all the more so when dynamic disturbances are presented.

2 Statement of the homicidal chauffeur game with a more agile pursuer

Let the dynamics in original coordinates be:

$$\begin{array}{lll} P: & \dot{x}_p = w\sin\theta & E: \quad \dot{x}_e = v_1 \\ & \dot{y}_p = w\cos\theta & \quad\;\; \dot{y}_e = v_2 \\ & \dot{\theta} = u & \\ & |u| \le 1,\ a \le w \le 1; & \quad\;\; |v| \le \nu. \end{array} \tag{4}$$

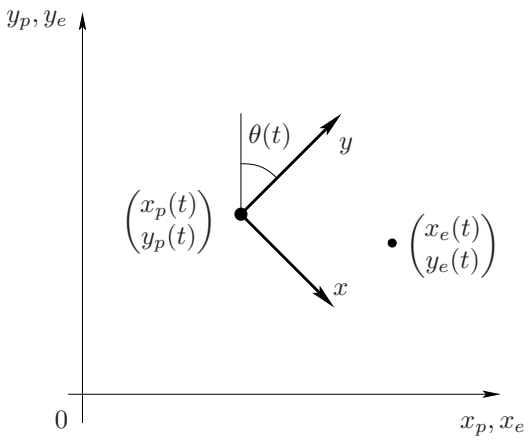

Figure 1: Movable reference system.

The constraint on the value of the angular velocity u does not depend on the magnitude of the linear velocity. The value w of the linear velocity can change instantaneously within the bounds $a \le w \le 1$, where a is a fixed parameter that fulfills the condition $a \in [-1, 1]$. The parameter ν in the constraint on the magnitude $|v|$ of the velocity $v = (v_1, v_2)'$ of player E is assumed to be from the interval $[0, 1)$.

The objective of player P is to capture player E in a closed circular neighborhood of radius r around his geometrical state as soon as possible.

Let us apply the reduced coordinates from ([10], pp. 29–30) which determine the relative position of player E in the rectangular coordinate system x, y with the origin at P and the axis y directed along the vector h, i.e., along the velocity vector of P computed for $w = 1$. The reduced coordinate system is explained in Fig. 1.

The dynamics (4) are transformed into:

$$\begin{aligned} \dot{x} &= -y\,u + v_x \\ \dot{y} &= \ \ x\,u - w + v_y \\ |u| &\le 1, \ \ a \le w \le 1, \ \ v = (v_x, v_y)', \ \ |v| \le \nu. \end{aligned} \tag{5}$$

In the reduced coordinates, the objective of player P is to bring the state (x, y) to a given terminal set M being a circle of the radius r with the center at the origin.

If $a = 1$, the dynamics (5) coincides with the homicidal chauffeur ones.

In the paper, numerically obtained level sets $W_\tau = \{(x, y) : \ V(x, y) \le \tau\}$ of the value function $V(x, y)$ of the time-optimal differential game with dynamics (5) will be presented. The structure of these sets depending on the parameter a will be explored.

The level sets are computed using an algorithm for solving time-optimal differential games developed by the authors [16].

3 Families of semipermeable curves

When solving differential games in the plane, it is useful to carry out a preliminary study of families of smooth semipermeable curves that are determined by the dynamics of the controlled system. The knowledge of these families for time-optimal problems allows to verify the correctness of the construction of barrier lines on which the value function is discontinuous.

A smooth semipermeable curve is a line with the following preventing property: one of the players can prevent crossing the curve from the positive side to the negative one, the other player can prevent crossing the curve from the negative side to the positive one.

Below, the notations

$$\mathcal{P} = \{(u, w) : \ |u| \le 1, \ w \in [a, 1]\}, \qquad \mathcal{Q} = \{v : |v| \le \nu\}$$

are used for the constraints on the controls of players P and E.

A. Consider the Hamiltonian

$$H(\ell, z) = \min_{\xi \in \mathcal{P}} \max_{v \in \mathcal{Q}} \ell' f(z, \xi, v), \quad z, \ell \in R^2. \tag{6}$$

Here,

$$f(z, \xi, v) = p(z)u + gw + v,$$

$$z = (x, y)', \quad \xi = (u, w)', \quad p(z) = (-y, x)', \quad g = (0, -1)'.$$

We study nonzero roots of the equation $H(\ell, z) = 0$, where $z \in R^2$ is fixed. Since the function $\ell \to H(\ell, z)$ is positively homogeneous, it is convenient to assume that $\ell \in \mathcal{E}$, where $\mathcal{E}$ is the circumference of unit radius centered at the origin.

Let $\ell, \ell_* \in \mathcal{E}, \ \ell \ne \ell_*$. The notation $\ell \prec \ell_*$ ($\ell \succ \ell_*$) means that the vector ℓ can be obtained from the vector ℓ_* using a counterclockwise (clockwise) rotation through an angle smaller than π. In fact, this order relation will be used only for vectors that are sufficiently close to each other.

Fix $z \in R^2$ and consider roots of the equation $H(\ell, z) = 0, \ \ell \in \mathcal{E}$. A vector ℓ_* is called the strict root "$-$" to "$+$" if there exist a vector $\kappa \in R^2$ and a neighborhood $S \subset \mathcal{E}$ of the vector ℓ_* such that $H(\ell_*, z) = \ell_*'\kappa = 0$ and $H(\ell, z) \le \ell'\kappa < 0$ ($H(\ell, z) \ge \ell'\kappa > 0$) for vectors $\ell \in S$ satisfying the relation $\ell \prec \ell_* \ (\ell \succ \ell_*)$. Similarly, the strict root "$+$" to "$-$" is defined through replacing $\ell \prec \ell_* \ (\ell \succ \ell_*)$ by $\ell \succ \ell_* \ (\ell \prec \ell_*)$. The roots "$-$" to "$+$" and "$+$" to "$-$" are called roots of the first and second type, respectively. In the following, when utilizing the notation $\ell \prec \ell_* \ (\ell \succ \ell_*)$ we will keep in mind that ℓ is from a neighborhood S like that mentioned in the definition of the roots.

Denote by $\Xi(\ell, z)$ the collection of all $\xi \in \mathcal{P}$ that provide the minimum in (6), that is:

$$\Xi(l, z) = \operatorname{argmin}\{\ell'(p(z)u + gw) : \xi \in \mathcal{P}\}.$$

If ℓ_* is a strict root of the first (second) type, take $\xi^{(1)}(\ell_*, z)$ $(\xi^{(2)}(\ell_*, z))$ equal to $\operatorname{argmin}\{\ell'(p(z)u + g\,w) : \xi \in \mathcal{P}(\ell_*, z)\}$, where $\ell \prec \ell_*$ $(\ell \succ \ell_*)$. Note that the result does not depend on the choice of ℓ. Let

$$v^{(1)}(\ell_*) = v^{(2)}(\ell_*) = \operatorname{argmax}\{\ell'_* v : v \in \mathcal{Q}\}.$$

Since $\mathcal{Q}$ is a circle, $v^{(i)}(\ell_*)$, $i = 1, 2$, is a singleton.

If ℓ_* is a root of the first type, consider the vectograms $f(z, \xi^{(1)}(\ell_*, z), \mathcal{Q})$, and $f(z, \mathcal{P}, v^{(1)}(\ell_*))$. We have

$$\ell' f(z, \xi^{(1)}(\ell_*, z), v) \le \max_{v \in \mathcal{Q}} \ell' f(z, \xi^{(1)}(\ell_*, z), v) = H(\ell, z) \le \ell'\kappa < 0 \qquad (7)$$

for $v \in \mathcal{Q}$ and $\ell \prec \ell_*$. For $\ell \succ \ell_*$, it holds:

$$\max_{v \in \mathcal{Q}} \ell' v \le \ell' v^{(1)}(\ell_*) + \ell'\kappa/2$$

because κ is orthogonal to ℓ_* (and hence to $v^{(1)}(\ell_*)$), and $\ell'\kappa > 0$. Thus,

$$H(\ell, z) \le \min_{\xi \in \mathcal{P}} \ell' f(z, \xi, v^{(1)}(\ell_*)) + \ell'\kappa/2.$$

The last inequality yields

$$\ell' f(z, \xi, v^{(1)}(\ell_*)) \ge \min_{\xi \in \mathcal{P}} \ell' f(z, \xi, v^{(1)}(\ell_*)) \ge H(\ell, z) - \ell'\kappa/2 \ge \ell'\kappa/2 > 0 \quad (8)$$

for $\xi \in \mathcal{P}$ and $\ell \succ \ell_*$.

Relations (7) and (8) ensure that the vectograms $f(z, \xi^{(1)}(\ell_*, z), \mathcal{Q})$, and $f(z, \mathcal{P}, v^{(1)}(\ell_*))$ do not contain zero and are located with respect to the direction of the vector $f^{(1)} = f(z, \xi^{(1)}(\ell_*, z), v^{(1)}(\ell_*))$, as it is shown in Fig. 2*a*.

Therefore, the existence of a strict root ℓ_* of the first type at a point z ensures together with taking the control $\xi^{(1)}(\ell_*, z)$ $(v^{(1)}(\ell_*))$ by player P (E) that the velocity vector $f(z, \xi^{(1)}(\ell_*, z), v)$ $(f(z, \xi, v^{(1)}(\ell_*)))$ is directed to the right (to the left) with respect to the direction of the vector $f^{(1)}$ for any control v (ξ) of player E (P). Such a disposition of the vectograms means that player P (E) guarantees the trajectories do not go to the left (to the right) with respect to the direction of $f^{(1)}$. The direction of the vector $f^{(1)}$ is called the semipermeable direction of the first type. The vector $f^{(1)}$ is orthogonal to the vector ℓ_*, its direction can be obtained from ℓ_* by a clockwise rotation through the angle $\pi/2$.

Arguing similarly, we obtain that the existence of a strict root ℓ_* of the second type at a point z ensures together with taking the control $\xi^{(2)}(\ell_*, z)$ $(v^{(2)}(\ell_*))$ by player P (E) that the velocity vector $f(z, \xi^{(2)}(\ell_*, z), v)$ $(f(z, \xi, v^{(2)}(\ell_*)))$ is directed to the left (to the right) with respect to the direction of the vector $f^{(2)} = f(z, \xi^{(2)}(\ell_*, z), v^{(2)}(\ell_*))$ for any control of player E (P). This means that player P (E) guarantees the trajectories do not go to the right (to the left) with respect to the direction of $f^{(2)}$. The direction of the vector $f^{(2)}$ is called

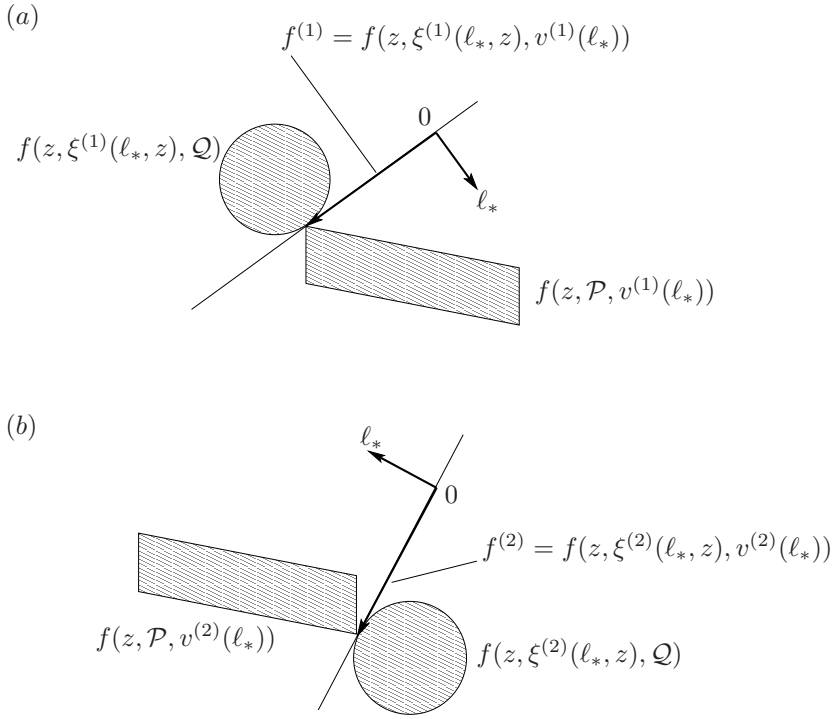

Figure 2: (a) Semipermeable direction of the first type. (b) Semipermeable direction of the second type.

the semipermeable direction of the second type. The vector $f^{(2)}$ is orthogonal to the vector ℓ_*, its direction can be obtained from ℓ_* by a counterclockwise rotation through the angle $\pi/2$ (see Fig. 2b).

Thus, there is a significant difference in the location of the vectograms for strict roots of the first and second type.

B. We distinguish semipermeable curves of the first and second types. A smooth curve is called semipermeable of the first (second) type if the direction of the tangent vector at any point along this curve is the semipermeable direction of the first (second) type.

The side of a semipermeable curve that player P (E) can keep is called positive (negative). The positive (negative) side of a semipermeable curve of the first type is on the right (on the left) when looking along the semipermeable direction. The opposite is valid for semipermeable curves of the second type.

Figure 3 illustrates the role of semipermeable curves of the first and second type in solving a game of kind with the classical homicidal chauffeur dynamics, the restriction $\mathcal{Q}$ is of a rather large radius. The objective of player P is to bring

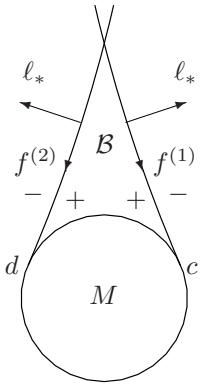

Figure 3: Semipermeable curves of the first and second type and capture set.

trajectories to the terminal set M which is a circle centered at the origin, the objective of player E is opposite. Denote by c and d the endpoints of the usable part [10] on the boundary of M. The semipermeable curves of the first and second type that are tangent to the set M and pass through the points c and d, respectively, define completely the capture set $\mathcal{B}$ of all points for which guaranteed time of attaining M is finite. The curves are faced towards each other with the positive sides.

C. In Fig. 4, the families of semipermeable curves for the classical homicidal chauffeur dynamics are presented. There are families $\Lambda^{(1),1}$ and $\Lambda^{(1),2}$ of the first type and families $\Lambda^{(2),1}$ and $\Lambda^{(2),2}$ of the second type. The second upper index in the notation $\Lambda^{(i),j}$ indicates those of two extremal values of control u that corresponds to this family: $j = 1$ is related to curves which are trajectories for $u = 1$; $j = 2$ is related to curves which are trajectories for $u = -1$. The arrows show the direction of motion in reverse time. Due to symmetry properties of the dynamics, all families can be obtained from only one of them (for example, $\Lambda^{(1),1}$) by means of reflections about the horizontal and vertical axes.

The construction of mentioned four families of smooth semipermeable curves can be explained as follows.

Let $a = 1$ in system (5). Assign the set

$$B_* = \{(x, y) : \ -y + v_x = 0, \ x - 1 + v_y = 0, \ v \in \mathcal{Q}\}$$

to the control $u = 1$, and the set

$$A_* = \{(x, y) : \ y + v_x = 0, \ -x - 1 + v_y = 0, \ v \in \mathcal{Q}\}$$

to the control $u = -1$. Hence, B_* is the set of all points in the plane x, y such that the velocity vector of system (5) for $w = 1$ vanishes at $u = 1$ and some $v \in \mathcal{Q}$. We have $A_* = -B_*$.

Consider two tangents to the sets A_*, B_* passing through the origin (see Fig. 5), and mark arcs $a_1a_2a_3$ and $b_1b_2b_3$ on ∂A_*, and ∂B_*, respectively.

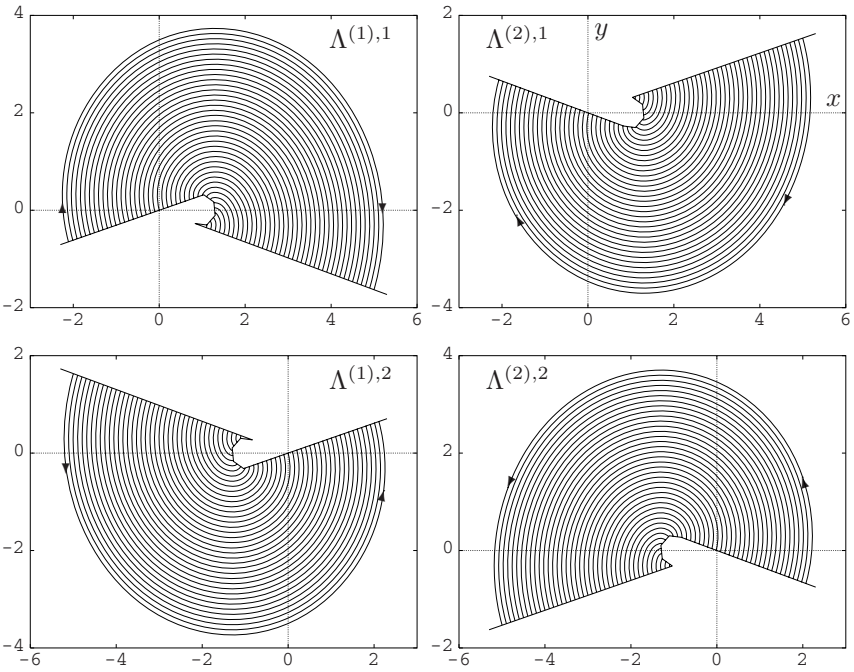

Figure 4: Families of smooth semipermeable curves for the classical homicidal chauffeur dynamics.

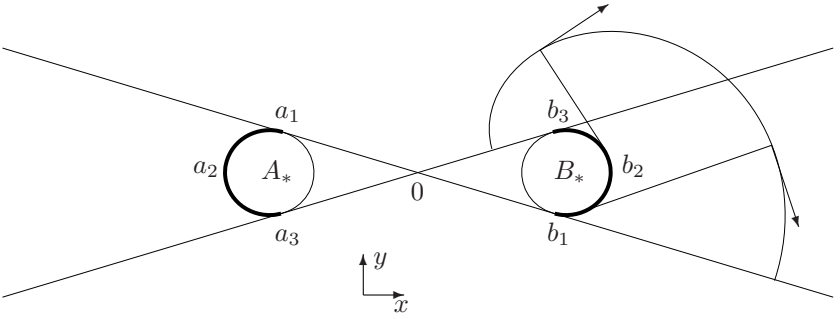

Figure 5: Auxiliary arcs generating the families of smooth semipermeable curves for the classical homicidal chauffeur dynamics.

Attach an inextensible string of a fixed length to the point b_1 and wind it up on the arc $b_1b_2b_3$. Then wind the string down keeping it taut in the clockwise direction. The end of the string traces an involute, which is a semipermeable curve of the family $\Lambda^{(1),1}$. A detailed proof of this fact is given in [17]. The complete family $\Lambda^{(1),1}$ is obtained by changing the length of the string.

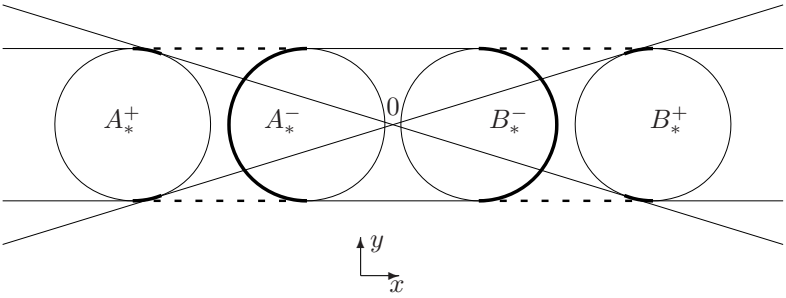

Figure 6: Auxiliary arcs generating the families of smooth semipermeable curves for dynamics (5); $a = 0.33$, $\nu = 0.3$.

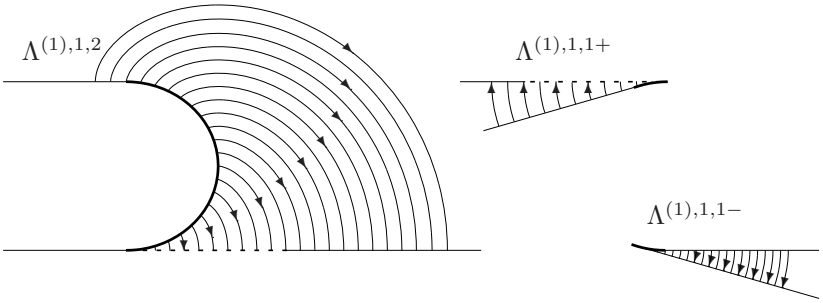

Figure 7: Three families of smooth semipermeable curves of the first type corresponding to $u = 1$ for dynamics (5); $a \geq -\nu$, $\nu = 0.3$.

The family $\Lambda^{(2),2}$ is obtained as the collection of the counterclockwise-involutes of the arc $a_1a_2a_3$ by attaching the string to the point a_3 .

The family $\Lambda^{(2),1}$ is generated by the clockwise-involutes of the arc $b_1b_2b_3$ provided the string is attached to the point b_3.

The family $\Lambda^{(1),2}$ is composed of the counterclockwise-involutes of the arc $a_1a_2a_3$ provided the string is attached to the point a_1.

D. Families of semipermeable curves corresponding to dynamics (5) are arranged in a more complicated way (see Figs. 6–10).

Figure 6 shows auxiliary lines used for the construction of the families. Here, A_*^+ and B_*^+ are the circles of radius ν with the centers at the points $(-1, 0)$ and $(1, 0)$, respectively. The circle A_*^+ (B_*^+) consists of all points (x, y) such that the right-hand side of system (5) becomes zero for $u = -1$ $(u = 1)$, $w = 1$, and some $v \in \mathcal{Q}$. The only difference in the definition of the circle A_*^- (B_*^-) is that $w = a$ instead of $w = 1$ is used. For Fig. 6, $a = 0.33$, $\nu = 0.3$. Six thick arcs on the boundaries of the circles are the only lines utilized for the construction of

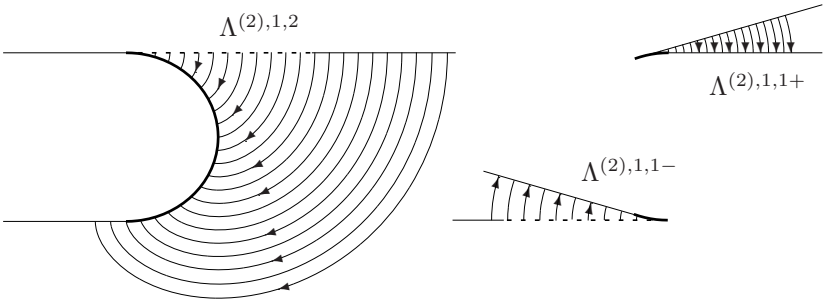

Figure 8: Three families of smooth semipermeable curves of the second type corresponding to $u = 1$ for dynamics (5); $a \geq -\nu$, $\nu = 0.3$.

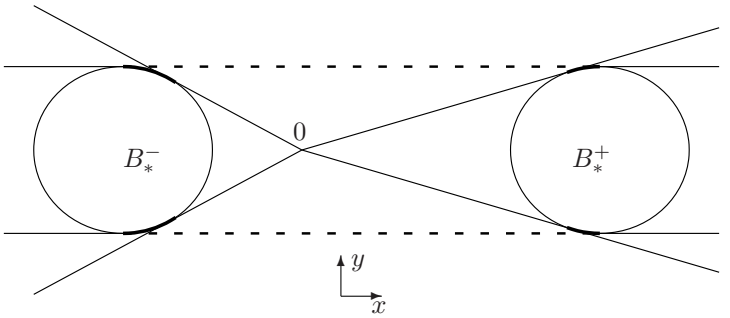

Figure 9: Auxiliary arcs generating the families of smooth semipermeable curves corresponding to $u = 1$ for dynamics (5); $a = -0.6$, $\nu = 0.3$.

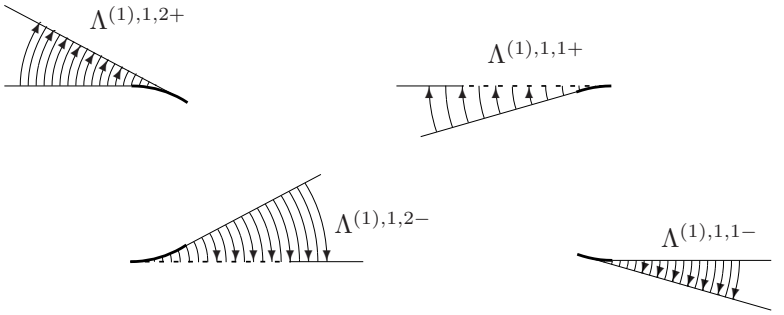

Figure 10: Four families of smooth semipermeable curves of the first type corresponding to $u = 1$ for dynamics (5); $a = -0.6$, $\nu = 0.3$.

families of smooth semipermeable curves.

In the problem considered, for $a \geq -\nu$, there are three families $\Lambda^{(1),1,1+}$, $\Lambda^{(1),1,1-}$, and $\Lambda^{(1),1,2}$ of semipermeable curves of the first type that correspond to $u = 1$ (instead of one family in the classical homicidal chauffeur problem). The families are drawn in Fig. 7. Every one of these three families consists of the involutes of one of the three arcs. The families $\Lambda^{(1),1,1+}$ and $\Lambda^{(1),1,2}$ overlap. There is also an overlap between the families $\Lambda^{(1),1,1-}$ and $\Lambda^{(1),1,2}$ over the part of the family $\Lambda^{(1),1,1-}$ in the region above the line $y = -\nu$. If $a \to 1$, the union of three families gives the family $\Lambda^{(1),1}$ of the classical homicidal chauffeur problem.

Figure 8 shows the families $\Lambda^{(2),1,1+}$, $\Lambda^{(2),1,1-}$, and $\Lambda^{(2),1,2}$ of the second type corresponding to $u = 1$. They are obtained by the reflection of corresponding families from Fig. 7 about the horizontal axis and by changing the direction of arrows. Families $\Lambda^{(2),2,1+}$, $\Lambda^{(2),2,1-}$, and $\Lambda^{(2),2,2}$ can be obtained by the reflection of corresponding families from Fig. 7 about the vertical axis (the direction of arrows does not change).

Families $\Lambda^{(1),2,1+}$, $\Lambda^{(1),2,1-}$, and $\Lambda^{(1),2,2}$ of the first type can be obtained by the reflection of families $\Lambda^{(2),1,1+}$, $\Lambda^{(2),1,1-}$, and $\Lambda^{(2),1,2}$ about the vertical axis.

For $-1 \leq a < -\nu$, the family $\Lambda^{(1),1,2}$ splits into two families: $\Lambda^{(1),1,2-}$ and $\Lambda^{(1),1,2+}$. Everything else is similar to the case $a \geq -\nu$. The lines that define the families of smooth semipermeable curves corresponding to $u = 1$ are depicted in Fig. 9. In Fig. 10, four families of the first type for $u = 1$ are presented.

4 Level sets of the value function

In this section, results of the computation of level sets W_τ of the value function $V(x, y)$ for time-optimal differential game with dynamics (5) will be presented. The collection of all points $(x, y) \in \partial W_\tau$ such that $V(x, y) = \tau$ is called the front corresponding to the reverse time τ. The computational procedure [16] for the construction of the level sets runs backward in time on the interval $[0, \tau_f]$. The value of τ_f is given below in the figure captions. For all figures, the horizontal axis is x, the vertical axis is y.

It is supposed in all examples that the set M is a circle of radius $r = 0.3$ with the center at the origin, and the control u is bounded as $|u| \leq 1$.

The following 6 variants of parameter values will be considered:

$$1.\ a=1, \quad 2.\ a = 0.25, \quad 3.\ a = -0.1, \quad 4.\ a=-0.4, \quad 5.\ a = -0.6, \quad 6.\ a = -1.$$

The variants are ordered by decreasing value of the parameter a. Remind that the constraint on the control w of player P is $a \leq w \leq 1$. Therefore, the capabilities of player P increase with the decrease of value a.

In every variant, the constraint on the control of player E is $|v| \leq \nu = 0.3$.

In the computations, the circle M is approximated by a regular 30-polygon, the circular constraint of player E is replaced by a regular octagon.

A. Let now describe level sets of the value function.

1) Figure 11 presents level sets W_τ for the classical homicidal chauffeur problem, variant 1. The value function is discontinuous on two barrier lines: the right barrier line is a semipermeable curve of the family $\Lambda^{(1),1}$, the left one is a semipermeable curve of the family $\Lambda^{(2),2}$ (see Fig. 4). The right barrier terminates at the lower tangent to the circle B_* passing through the origin, the left one terminates at the lower tangent to the circle A_*. After the termination, the barriers are continued by the lines formed of the corner points on the fronts of level sets. The value function is not differentiable on these lines.

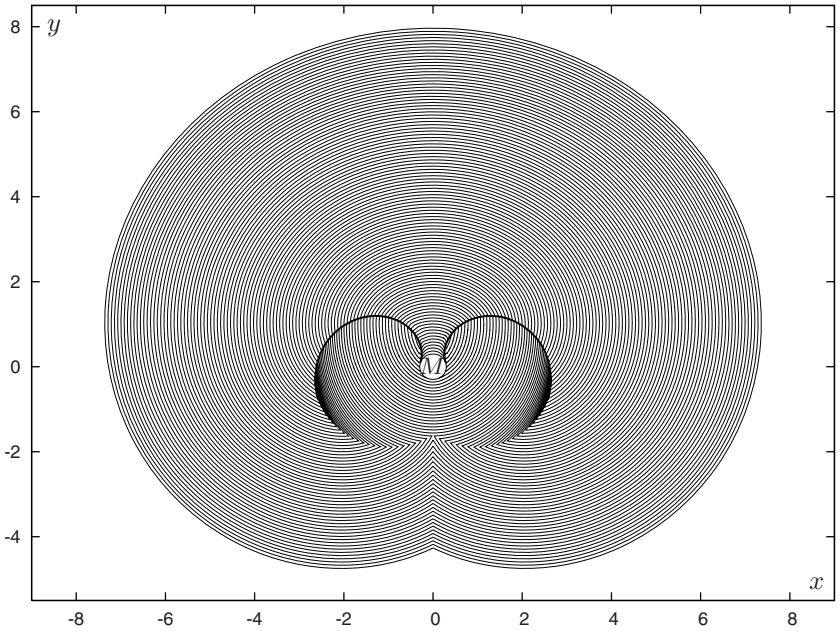

Figure 11: Level sets W_τ for the classical homicidal chauffeur problem; $\tau_f = 10.3$.

We can conclude about lines of discontinuity of the value function by analyzing the families of semipermeable curves before the construction of level sets of the value function. The knowledge of these families is utilized for the verification of numerical computation of level sets.

After bending round the right and left barriers, the right and left parts of the front meet on the vertical axis at time $\tau = 7.82$. A closed front occurs and a hole is generated which is completely filled out at time $\tau = 10.3$.

2) If $a \geq -\nu = -0.3$, then there is only one usable part on the boundary ∂M for the chosen radius $r = 0.3$ of the terminal circle M. It is located in the upper part of ∂M. Its right (left) endpoint is the intersection point of ∂M with the upper

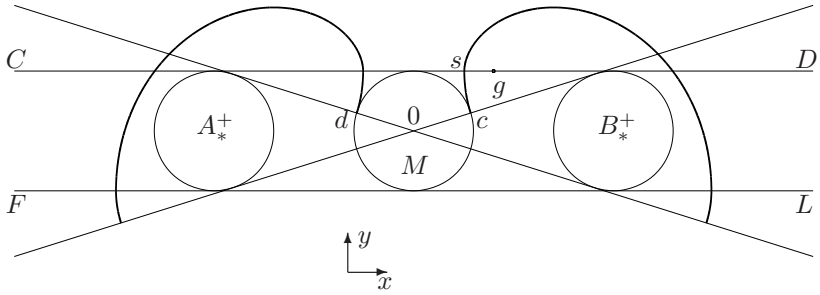

Figure 12: Long barrier emanating from the point c.

tangent to B_*^+ (A_*^+) passing through the origin. In Fig. 12, c and d are the endpoints of the usable part (from which the fronts are emitted in the backward procedure).

For chosen values $r = 0.3$ and $\nu = 0.3$, there exists a value $\bar{a} \in (0, 1)$ of the parameter a which separates the case of a "long" barrier from the case of a "short" one. The barrier lines emanate from the points c and d of the usable part. Due to the symmetry of the solution with respect to the vertical axis, one can only consider the right barrier emanating from the point c. The right long barrier is a semipermeable curve obtained by a smooth junction of a curve of the family $\Lambda^{(1),1,1+}$ going backward in time from the point c with a curve of the family $\Lambda^{(1),1,2}$ and, later on, with a curve of the family $\Lambda^{(1),1,1-}$ (see Fig. 7). The first junction can occur on the horizontal line $y = \nu = 0.3$ (denote it by CD), the second one is on the horizontal line $y = -\nu = -0.3$ (denote it by FL). The right and left long barriers are shown in Fig. 12. The right short barrier consists of a curve of the family $\Lambda^{(1),1,1+}$ going backward in time from the point c up to the line CD.

If the intersection point s of the last-mentioned semipermeable curve with the line CD is to the left from the point $g = (a, \nu)'$, being a tangent point of the line CD and the set B_*^-, then the barrier can be continued by a curve of the family $\Lambda^{(1),1,2}$. Therefore, we obtain a long barrier. If the point s is to the right from g, there is no any extension. In this case, a short barrier occurs. The coincidence $s = g$ defines a critical value $\bar{a}$. The transient case $a = \bar{a}$ is of great theoretical importance.

The value $a = 0.25$ in variant 2 is close to $\bar{a}$. The results of the computation of sets W_τ for this variant are presented in Fig. 13. The obtained right and left barriers are long. Since in the computation the constraint $|v| \le \nu$ is a regular octagon, the sets B_*^+, B_*^-, A_*^+, and A_*^- are octagons as well. Figure 14 shows an enlarged fragment of Fig. 13 with additionally drawn sets A_*^+ and A_*^-.

3) Figure 15 presents computation results for variant 3. Enlarged fragments of Fig. 15 are shown in Figs. 16 and 17.

Here, the right barrier that emanates from the right endpoint c of the usable part on ∂M belongs to the family $\Lambda^{(1),1,1+}$. In the notations of Fig. 12, the point s is to the right of the point g that results in the short barrier. The left barrier

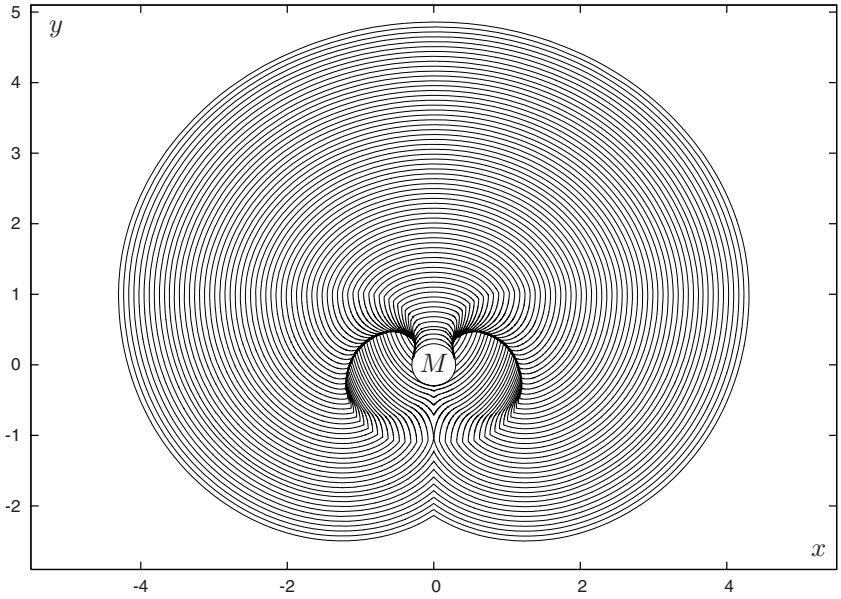

Figure 13: Level sets W_τ for differential game (5); $a = 0.25$, $\tau_f = 6.7$.

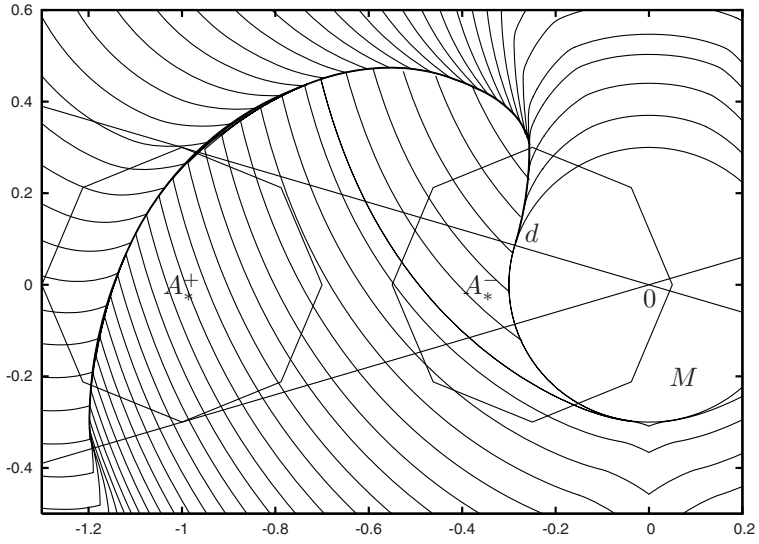

Figure 14: Enlarged fragment of Fig. 13.

which is symmetrical to the right one with respect to the vertical axis belongs to the family $\Lambda^{(2),2,1+}$. The termination of barriers on the horizontal line $y = 0.3$

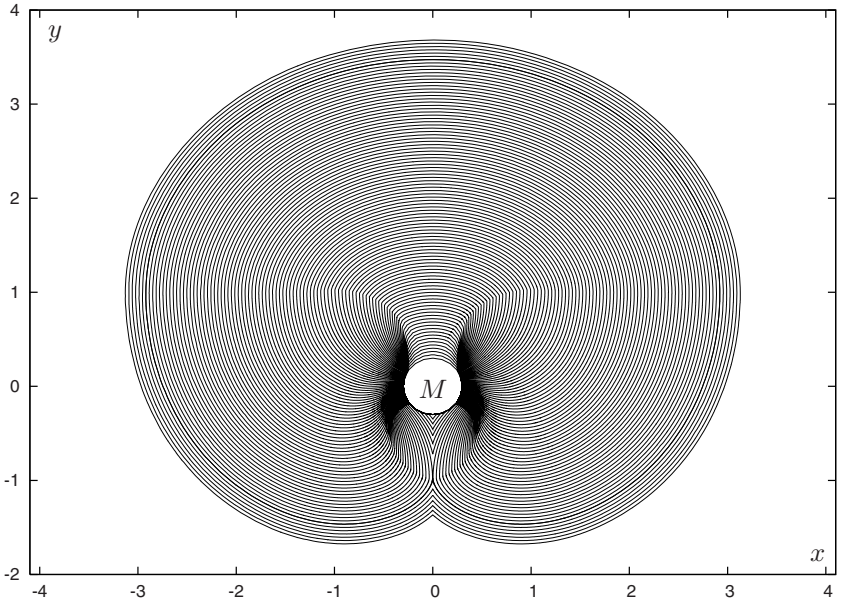

Figure 15: Level sets W_τ for differential game (5); $a = -0.1$, $\tau_f = 4.89$.

is completely in accordance with the results that follow from the knowledge of families of semipermeable curves.

After bending round the barrier lines, the ends of the front go down along the negative sides of the barriers and then move along the boundary of the terminal set. This is well seen in Figs. 16 and 17. Parts of the front near the right and left sides of the terminal set and far from it move with different velocities, which yields the generation of the right and left singular lines where the value function is non-differentiable.

Values τ_f given in the captions of Figs. 11, 13, and 15 correspond to the time instants at which the "inner hole" is filled out with the fronts.

4) Consider variant 4 (see Figs. 18 and 19). For this variant, two usable parts on ∂M arise. The upper usable part is larger than the lower one.

The right and left barriers emanating from the endpoints of the upper usable part are semipermeable curves of the families $\Lambda^{(1),1,1+}$ and $\Lambda^{(2),2,1+}$, respectively. They terminate, as expected, on the horizontal line $y = 0.3$. Outside set M, the value function is discontinuous on these two lines only.

The ends of the fronts which propagate from the lower usable part move very slowly along ∂M (see Fig. 20a). At some time, a local non-convexity with a kink is formed on a going down front. This kink rises upwards and after some time it

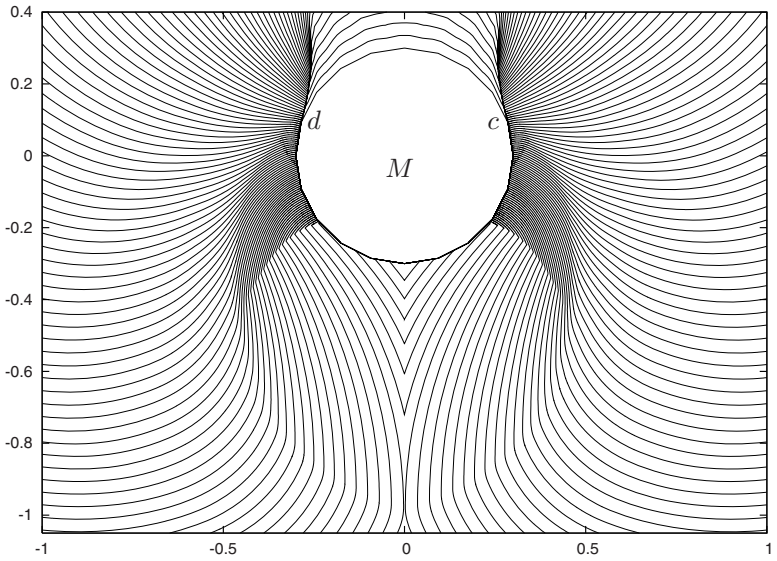

Figure 16: Enlarged fragment of Fig. 15.

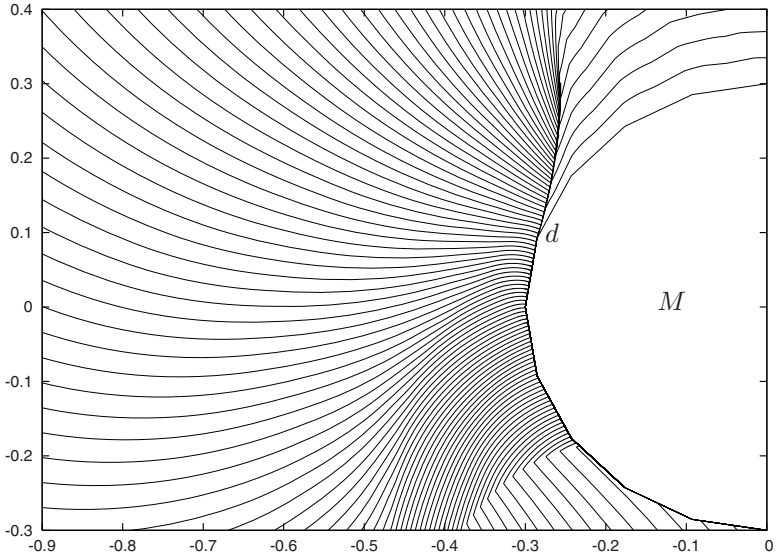

Figure 17: One more enlarged fragment of Fig. 15.

reaches the endpoint of the front on ∂M. In fact, a new endpoint of the front that moves along ∂M faster than before arises. Then, after some time, this endpoint

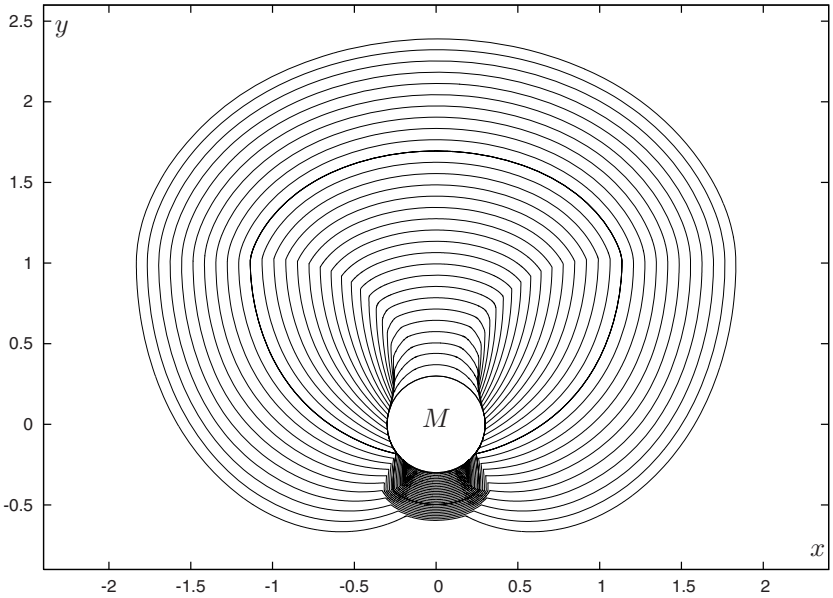

Figure 18: Level sets W_τ for differential game (5); $a = -0.4$, $\tau_f = 3$.

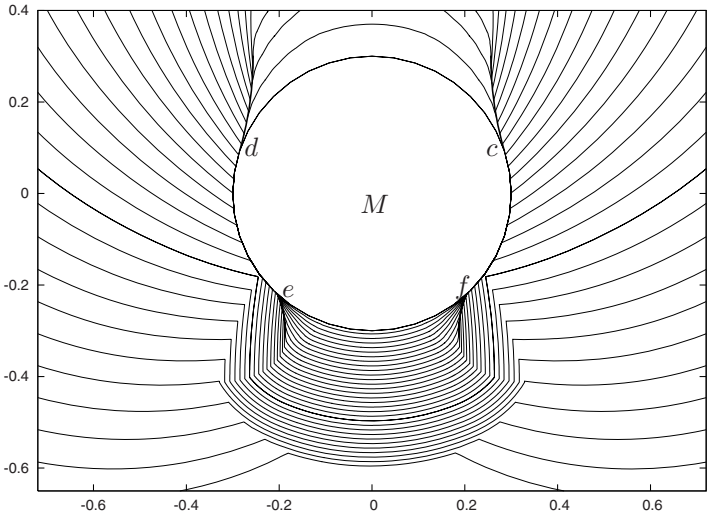

Figure 19: Enlarged fragment of Fig. 18.

meets the endpoint of the front going down along ∂M. A closed front is formed (Fig. 19).

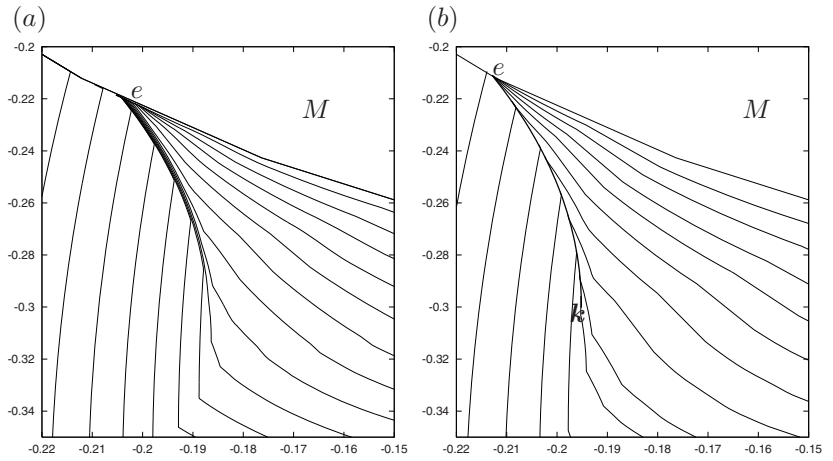

Figure 20: Continuous and discontinuous value function. (a) Enlarged fragment of Fig. 19, $a = -0.4$. The region of fronts accumulation is shown. The value function is continuous outside set M. (b) Level sets for $a = -0.425$. The value function is discontinuous outside set M on the barrier line ek.

5) For $a \le \tilde{a} = -0.3\sqrt{2}$, there are barrier lines that emanate from the endpoints of the lower usable part and terminate at the horizontal straight line $y = -\nu = -0.3$. The left barrier line is a semipermeable curve of the family $\Lambda^{(1),1,2-}$, the right one is a semipermeable curve of the family $\Lambda^{(2),2,2-}$.

Figure 20b computed for $a = -0.425$ shows the lower fronts bending round the left barrier line. This can be compared with Fig. 20a computed for $a = -0.4$. At first sight, the pictures are very similar. However, the value function in Fig. 20b is discontinuous on the barrier line ek, while the value function in Fig. 20a is continuous in a similar region below the set M.

The behavior of lower fronts for values a close to $\tilde{a}$ initiates the following question which, to our opinion, can hardly be answered based on numerics only. Is it true that for $a = -0.3\sqrt{2}$ the endpoints of the lower fronts stay at the endpoints e, f of the usable part till some time $\hat{\tau} > 0$ and only for $\tau > \hat{\tau}$ begin to go down along the barrier lines?

Figures 21 and 22 show level sets of the value function for $a = -0.6$ (variant 5). Fronts generated by the upper and lower usable parts encounter at some time $\tau_* = 1.41$ (see Fig. 22). For $\tau > \tau_*$, the computation continues from the closed front.

6) For $a = -1$ (variant 6 being shown in Fig. 23), the computed sets are symmetrical with respect to both horizontal axis x and vertical axis y. Two short upper barrier lines like in variants 3, 4, and 5 are present. The lower barrier lines are symmetrical to the upper ones with respect to the axis x.

Note that, for $\nu = 0$, the set W_τ coincides with the reachable set $G(t, M)$ of

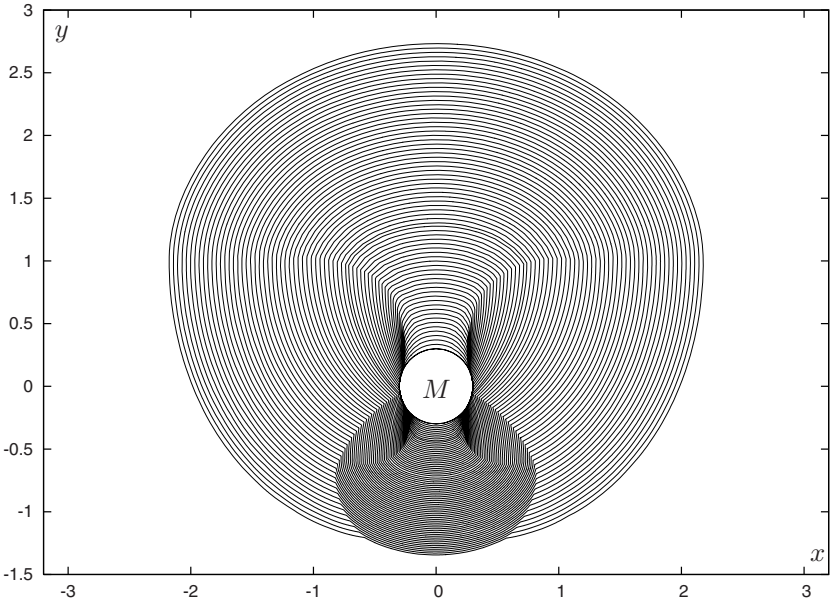

Figure 21: Level sets W_τ for differential game (5); $a = -0.6$, $\tau_f = 3.5$.

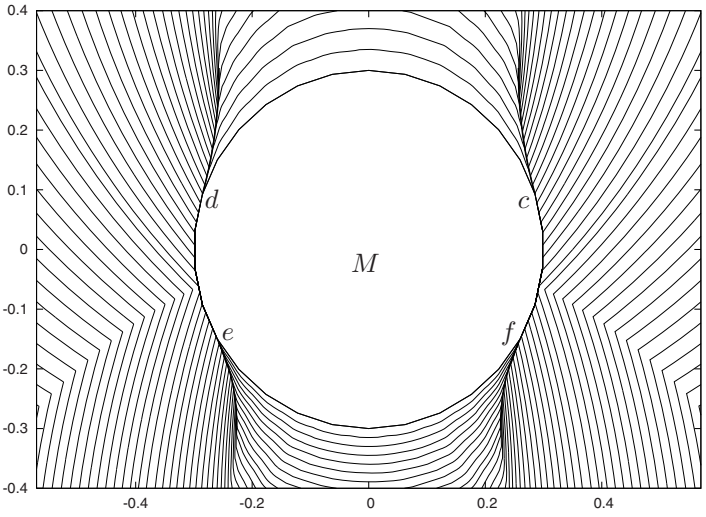

Figure 22: Enlarged fragment of Fig. 21.

system (3) in the plane of geometric coordinates at time $t = \tau$ with M being the initial set and with initial orientation of the forward motion direction h along

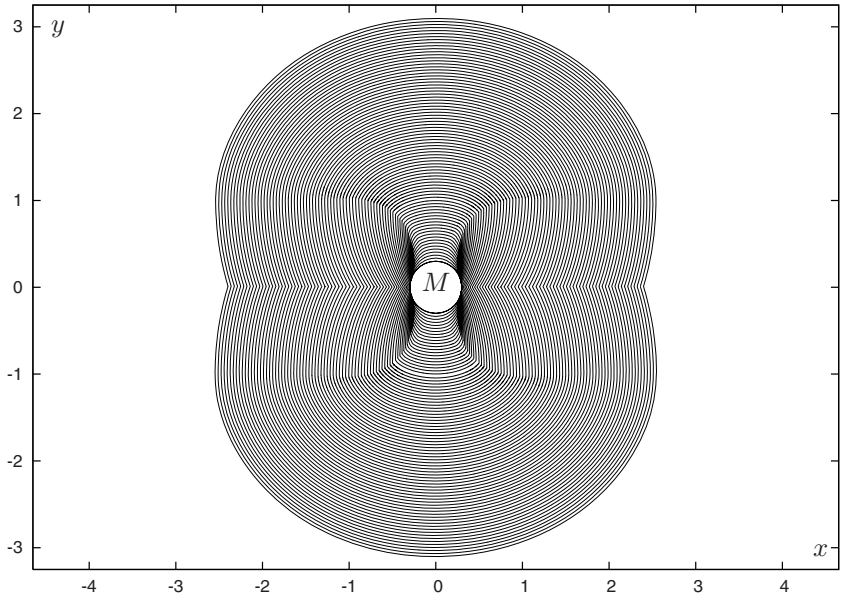

Figure 23: Level sets W_τ for differential game (5); $a = -1$, $\tau_f = 4$.

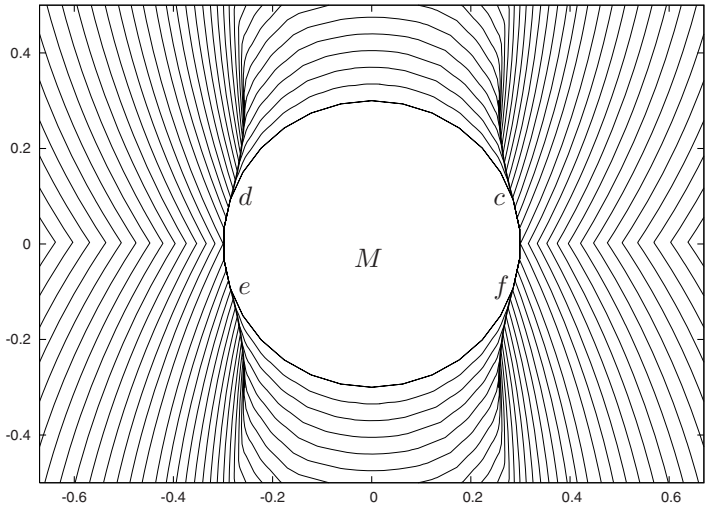

Figure 24: Enlarged fragment of Fig. 23.

the vertical axis. For Reeds and Shepp's model and the point set $M = \{0\}$, the boundary $\partial G(t, \{0\})$ is well investigated analytically in [21]. Besides, the structure

of open-loop controls $u(\cdot)$, $w(\cdot)$ that bring the system to $\partial G(t, \{0\})$ is established. The sets W_τ shown in Fig. 23 are similar to the ones in Fig. 7 from [21]. But, to our opinion, the principal, and important fact for applications is that the optimal guaranteed time (the value function $V(x, y)$) is not continuous if disturbances are presented (i.e., $\nu > 0$). If $\nu = 0$, the value function is continuous.

The numerical procedure utilized for the computation of all level sets presented above uses an automatic adjustment of the step width Δ of the backward construction. The initial value of Δ, which is usually equal to 0.01, can decrease up to 10 times in the course of construction. The fronts are shown with the time step 0.1 in Figs. 11, 13, 14, 18–20, and with the time step 0.05 in Figs. 15–17, Figs. 21–24.

B. In Fig. 25, level sets W_τ computed for $\tau = 1$ are presented. Five sets are shown that correspond to the following values of parameter a: $1, 0.25, -0.1, -0.6, -1$. One can see how the set W_τ grows with the decrease of a, i.e., with the increasing length of the interval $[a, 1]$ from which the control w is being chosen. For $a = 1, 0.25, -0.1$, the set W_τ consists of an upper piece only; for $a = -0.6, -1$, a lower piece is added. The upper and lower pieces are symmetrical for $a = -1$.

Level sets $W(\tau)$ for $\tau = 3$ are given in Fig. 26.

Figures 25 and 26 demonstrate not only the dependence of the size of sets W_τ on the parameter a. The boundary of every set from Fig. 25 ($\tau = 1$) and every set from Fig. 26 ($\tau = 3$) contains the common upper smooth arc mn. This means that the optimal feedback control of player P for initial points on mn is the same as in the classical game, i.e., $w \equiv 1$. Any other common arcs on ∂W_τ do not exist. Therefore, for those initial points on ∂W_τ which do not belong to the arc mn, the optimal control of player P should utilize both the value $w = 1$ and $w = a$. The construction of optimal feedback control of player P on the base of level sets of the value function is a separate question which is not discussed in this paper. For Reeds and Shepp's problem (i.e., for $a = -1$), the optimal feedback control in the absence of disturbances (i.e., for $\nu = 0$) has been constructed in papers [22], [23].

C. Figure 27 demonstrates the discontinuity curves of the value function depending on the parameter a. As it was already mentioned, the upper usable part defined by the points c and d on the boundary of the circle M is the same for all values $a \in [-1, 1]$. The right and left barrier lines emanate from the points c and d. For $a \in [\overline{a}, 1]$, where $\overline{a} \approx 0.25$, we have long barriers (Fig. 27a). For $a \in [-1, \overline{a})$, the barriers are short (Fig. 27b). The short barriers terminate on the horizontal line $y = \nu = 0.3$. For $a \in [-0.3, 1]$, the lower part of the boundary of the circle M between the points c and d is a discontinuity curve of the value function.

If $a \in [-1, -0.3)$, there is a lower usable part ef (Fig. 27b) on the boundary of the circle M, which increases with decreasing a. The arcs cf and de on ∂M are discontinuity curves of the value function. If $a \in (\tilde{a}, -0.3)$, where $\tilde{a} = -0.3\sqrt{2}$, barrier lines emanating from the points e and f do not exist. For $a \in [-1, \tilde{a}]$, there is a barrier line being a first type semipermeable curve of the family $\Lambda^{(1),1,2-}$ that emanate from the left endpoint e of the usable part. The curve terminates on the horizontal line $y = -\nu = -0.3$. The right barrier emanated from the point f is

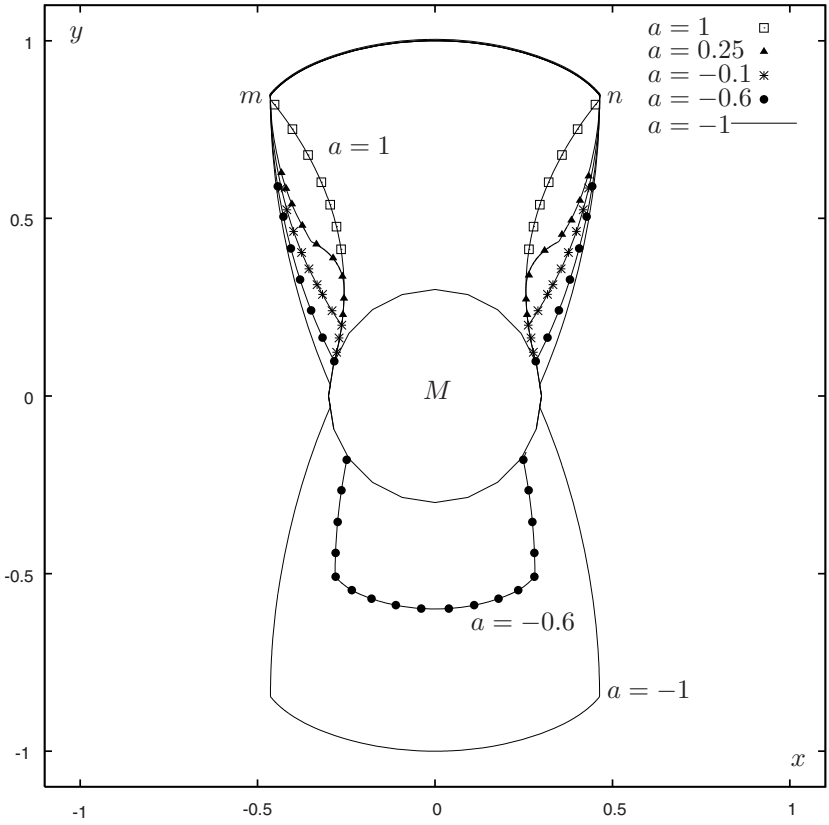

Figure 25: Level sets $W_\tau, \tau = 1$, of the value function for various magnitudes of the parameter a.

symmetrical to the left one with respect to the vertical axis and is a second type semipermeable curve.

5 Conclusion

It is known that the optimal control problems with dynamics describing an inertial car (see, e.g., [11]) are very complicated to study. This is why simplified models are widely used in mathematical literature. In particular, Reeds and Shepp's model is popular enough.

It is assumed in this model that the car can change instantaneously not only the angular velocity but also the direction of its motion to the opposite one without any loss in the velocity.

Therefore, we have two controls. The first control u is bounded as $|u| \leq 1$ and defines the angular velocity, the second control $w = \pm 1$ specifies the direc-

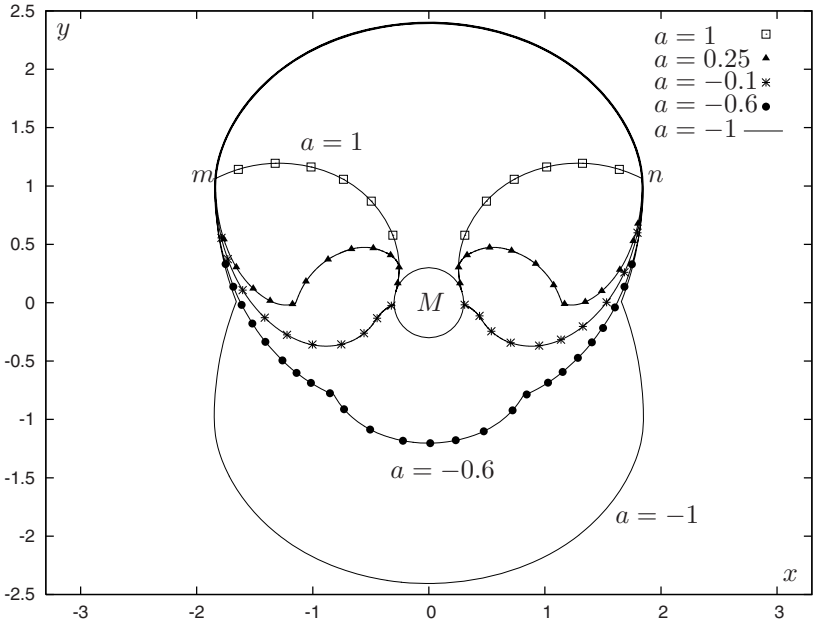

Figure 26: Level sets $W_\tau, \tau = 3$, of the value function for various magnitudes of the parameter a.

tion of motion. Using the convexification of vectograms, we can replace the constraint $w = \pm 1$ by the constraint $|w| \leq 1$. Thus, we can speak about an instantaneous change of the linear velocity in the range from -1 to $+1$ for Reeds and Shepp's model.

It is supposed in the paper that control w which instantaneously changes the magnitude of the linear velocity is restricted as $a \leq w \leq 1$. Here, $a \in [-1, +1]$ is the parameter of the problem. For $a = 1$, we have the car with the constant magnitude of the linear velocity. For $a = -1$, we obtain Reeds and Shepp's car.

Using the above-mentioned dynamics of the car, we investigate a differential game which is similar to the famous homicidal chauffeur game by R. Isaacs. The objective of the player P that controls the car is to catch as soon as possible a non-inertial pedestrian E in a given circular neighborhood of P-state. For $a = 1$, this game becomes the classical one.

After we applied Isaacs' transformation, the construction of level sets of the value function is run in the two-dimensional plane of reduced coordinates. The level sets are computed using the algorithm developed by the authors for time-optimal differential games in the plane. This algorithm enables to construct the level sets of the value function (in other words, the fronts or isochrones) with good accuracy, which allows us to investigate in detail the regions of accumulation of fronts, the discontinuity lines of the value function, and the behavior of fronts near

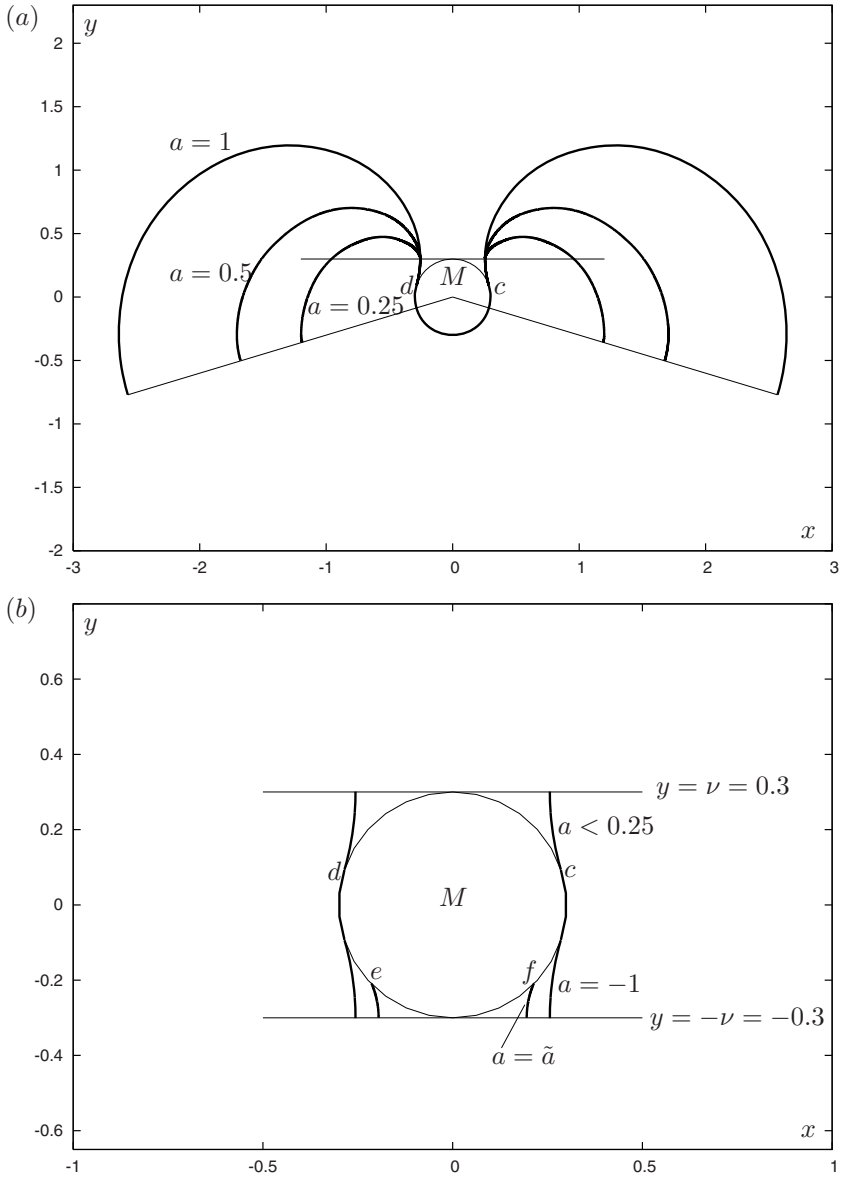

Figure 27: Discontinuity lines of the value function depending on the parameter a; (a) $a \geq \overline{a} \approx 0.25$; (b) $a < \overline{a}$.

such lines. In the paper, the structure of level sets is analyzed depending on the parameter a .

Additionally and independently on the construction of level sets of the value

function, the families of smooth semipermeable curves defined by the dynamics of the problem are described in the plane of reduced coordinates. The knowledge of these families enables to validate the discontinuity lines computed in the course of run of the algorithm for the construction of level sets. Since the families of semipermeable curves depend on the dynamics only, they can be also used in other problems with mentioned dynamics, for example, in time-optimal problems with objectives of the players that are different from those considered in this paper.

Acknowledgements

This research was supported by RFBR Grants Nos. 06-01-00414 and 07-01-96085.

References

[1] Bardi M., Falcone M., Soravia P., *Numerical methods for pursuit-evasion games via viscosity solutions*, in M. Bardi, T.E.S. Raghavan, T. Parthasarathy (eds.), *Stochastic and Differential Games: Theory and Numerical Methods. Annals of the International Society of Dynamic Games* **4**, Birkhäuser, Boston, (1999), 105–175.

[2] Bernhard P., Larrouturou B., *Etude de la barriere pour un probleme de fuite optimale dans le plan*, Rapport de Recherche, INRIA, Sophia-Antipolis, (1989).

[3] Boissonnat J. D., Cerezo A., Leblond J., *Shortest paths of bounded curvature in the plane*, Proc. IEEE Conf. Robotics and Automation, Nice, France, (1992).

[4] Breakwell J. V., Merz A. W., *Toward a complete solution of the homicidal chauffeur game*, Proc. of the 1st Int. Conf. on the Theory and Applications of Differential Games, Amherst, Massachusetts, (1969).

[5] Breakwell J. V., *Zero-sum differential games with terminal payoff*, in P. Hagedorn, H. W. Knobloch, G. J. Olsder (eds.), *Differential Games and Applications. Lecture Notes in Control and Information Sciences*, Springer, Berlin, (1977), 70–95.

[6] Cardaliaguet P., Quincampoix M., Saint-Pierre P., *Numerical methods for optimal control and differential games*, Ceremade CNRS URA 749, University of Paris-Dauphine, (1995).

[7] Cockayne E. J., Hall G. W. C., *Plane motion of a particle subject to curvature constraints*, SIAM J. Control **13**(1), (1975), 197–220.

[8] Dubins L. E., *On curves of minimal length with a constraint on average curvature and with prescribed initial and terminal positions and tangents*, Amer. J. Math. **79**, (1957), 497–516.

[9] Isaacs R., Games of pursuit, Scientific report of the RAND Corporation, Santa Monica, (1951).

[10] Isaacs R., *Differential Games*, John Wiley, New York, (1965).

[11] Laumond J.-P. (ed.), *Robot Motion Planning and Control*, Lecture Notes in Control and Information Sciences **229**, Springer, New York, (1998).

[12] Lewin J., Breakwell J. V., *The surveillance-evasion game of degree*, JOTA **16**(3/4), (1975), 339–353.

[13] Lewin J., Olsder, G. J., *Conic surveillance-evasion*, JOTA **27**(1), (1979), 107–125.

[14] Markov A. A., *Some examples of the solution of a special kind of problem on greatest and least quantities*, Soobscenija Charkovskogo matematiceskogo obscestva, Ser.2,1, NN5,6, (1889), 250–276 (in Russian).

[15] Merz A. W., *The homicidal chauffeur – a differential game*, PhD Thesis, Stanford University, (1971).

[16] Patsko V. S., Turova V. L., *Level sets of the value function in differential games with the homicidal chauffeur dynamics*, Int. Game Theory Review **3**(1), (2001), 67–112.

[17] Patsko V. S., Turova V. L., *Families of semipermeable curves in differential games with the homicidal chauffeur dynamics*, Automatica **40**(12), (2004), 2059–2068.

[18] Pecsvaradi T., *Optimal horizontal guidance law for aircraft in the terminal area*, IEEE Trans. on Automatic Control **AC-17**(6), (1972), 763–772.

[19] Raivio T., Ehtamo H., *On the numerical solution of a class of pursuit-evasion games*, in J. Filar, K. Mizukami, V. Gaitsgory (eds.), *Advances in Dynamic Games and Applications. Annals of the International Society of Dynamic Games* **5**, Birkhäuser, Boston, (2000), 177–192.

[20] Reeds J. A., Shepp L. A., *Optimal paths for a car that goes both forwards and backwards*, Pacific J. Math. **145**(2), (1990), 367–393.

[21] Souères P., Fourquet J.-Y., Laumond J.-P., *Set of reachable positions for a car*, IEEE Trans. on Automatic Control **39**(8), (1994), 1626–1630.

[22] Souères P., Laumond J-P., *Shortest paths synthesis for a car-like robot*, IEEE Trans. on Automatic Control **41**(5), (1996), 672–688.

[23] Souères P., *Minimum-length trajectories for a car: an example of the use of Boltianskii's sufficient conditions for optimality*, IEEE Trans. on Automatic Control **52**(2), (2007), 323–327.

[24] Sussmann H. J., Tang W., *Shortest paths for the Reeds-Shepp car: a worked*

out example of the use of geometric techniques in nonlinear optimal control, Rutgers University, New Brunswick, NJ, Rep. SYCON-91-10, (1991).

[25] Vendittelli M., Laumond J.-P., Nissoux C., *Obstacle distance for car-like robots*, IEEE Trans. on Robotics and Automation **15**(4), (1999), 678–691.